

Janssen 2.0: Audio Inpainting in the Time-frequency Domain

Ondřej Mokrý

Dept. of Telecommunications
Brno University of Technology
Czech Republic
ondrej.mokry@vut.cz

Peter Balušk

Dept. of Telecommunications
Brno University of Technology
Czech Republic
230531@vut.cz

Pavel Rajmic

Dept. of Telecommunications
Brno University of Technology
Czech Republic
pavel.rajmic@vut.cz

Abstract—The paper focuses on inpainting missing parts of an audio signal spectrogram. First, a recent successful approach based on an untrained neural network is revised and its several modifications are proposed, improving the signal-to-noise ratio of the restored audio. Second, the Janssen algorithm, the autoregression-based state-of-the-art for time-domain audio inpainting, is adapted for the time-frequency setting. This novel method, coined Janssen-TF, is compared to the neural network approach using both objective metrics and a subjective listening test, proving Janssen-TF to be superior in all the considered measures.

Index Terms—audio inpainting, autoregression, deep prior, spectrogram.

I. INTRODUCTION

Audio inpainting, sometimes referred to as missing audio interpolation or concealment, is the task of filling in the absent parts of audio with a meaningful content. Typically, the missing information is in the form of lost samples in the time domain. If compact regions of such samples are present, they are often referred to as the gaps. For the described task, plenty of methods have been developed: those based on the autoregressive character of audio [1], [2], methods based on the sparsity of the time-frequency representation of audio [3], [4], [5], [6], or methods relying on similarities in audio recordings [7], [8], [9]. Quite recently, deep learning audio inpainting methods appeared [10], [11]. For gaps of up to 50 ms in length, the Janssen method [2], [12] has been evaluated the best for a long time, but PHAIN [13] may become a new state-of-the art.

The time-domain inpainting represents the most natural case from the point of view of practical applications (signal recovery). Nonetheless, many practical algorithms, such as the classic audio coding algorithms (MP3, AAC, etc.), operate on short-time signal spectra. From this perspective, it is valuable to think about inpainting in the time-frequency domain.¹ In such a case, a portion of time-frequency (TF) coefficients² are missing, which need to be recovered to allow a later

The work was supported by the Czech Science Foundation (GAČR) Project No. 23-07294S. The authors are grateful to NVIDIA for their donation of the Titan XP graphic card, which has been used in this research.

¹In other fields, one can go even further and require inpainting purely in the frequency domain, see for example [14], [15].

²typically in the form of a complex-valued matrix

reconstruction of the time-domain signal. Indeed, there have been a few methods developed in the TF context, all of them relying on neural modeling [16], [17], [18]. The most recent work [18] is based on the concept of a “deep prior”, a neural network that does not require training in the common sense.

Note that a compact gap in time bears some fundamental differences compared with a gap in the form of missing a number of consecutive columns of a spectrogram. This follows from the nature of time-frequency transforms, which use windows with overlaps to compute spectrograms, see for instance [19]. In particular, a gap in a spectrogram does not fully correspond to a time-domain gap and vice versa; there is always an amplitude fading in one of the domains.

The goal of this paper is to adopt the Janssen algorithm [2], proven successful in the time-domain case, to the TF-domain case, and compare its performance with the recent deep-prior-based approach of [18], both using objective metrics and by listening tests.

II. DEEP PRIOR AUDIO INPAINTING (DPAI)

The deep prior, introduced in [20], is a concept used for the reconstruction of corrupted signals using an “untrained” convolutional neural network (CNN). The signal reconstruction involves only a proper CNN architecture and the corrupted signal. The deep prior concept has also proven that the network architecture matters much more than previously thought.

A. Application of Deep Prior to Audio Inpainting

Deep prior reconstruction can be utilized in a variety of applications [20]. In the context of the time-domain audio inpainting, consider a corrupted signal $\mathbf{x}^{\text{cor}} \in \mathbb{R}^N$, having missing regions (filled with zeros), compared with the original signal $\mathbf{x}^{\text{orig}} \in \mathbb{R}^N$. Formally, if a binary mask $\mathbf{m} \in \{0, 1\}^N$ is utilized to represent the missing sections of the signal, the relation $\mathbf{x}^{\text{cor}} = \mathbf{m} \odot \mathbf{x}^{\text{orig}}$ holds, where \odot represents the elementwise product. Such a relation naturally characterizes the feasible set $\mathcal{F}_T = \{\mathbf{x} \mid \mathbf{m} \odot \mathbf{x} = \mathbf{m} \odot \mathbf{x}^{\text{orig}}\}$.

An encoder–decoder CNN denoted $f_{\theta}(\mathbf{n})$ is assumed to be able to generate *any* signal of size N using a random but fixed noise input $\mathbf{n} \in \mathbb{R}^N$, using a proper θ . This is a reliable assumption since the number of network parameters θ (weights and biases) is significantly greater than N .

In the deep prior reconstruction, parameters θ are initialized randomly. To obtain a reconstruction result, θ is then optimized as follows:

$$\theta^* = \operatorname{argmin}_{\theta} E(\mathbf{m} \odot f_{\theta}(\mathbf{n}), \mathbf{x}^{\text{cor}}), \quad (1)$$

where E is a differentiable data fidelity function measuring the closeness of its two inputs. The optimal θ^* can be obtained using an iterative optimizer, e.g., Adam [21]. The crucial observation is that the optimization must be interrupted before it reaches θ^* , for which we would have $f_{\theta^*}(\mathbf{n}) = \mathbf{x}^{\text{cor}}$. Instead, early stopping of the training process is desired, resulting in an estimate $\hat{\theta}$ and a corresponding $\hat{\mathbf{x}} = f_{\hat{\theta}}(\mathbf{n})$ [20].

The authors of [18] used an analog approach to inpaint audio in the transformed domain. Through the use of the short-time Fourier transform (STFT), an audio recording \mathbf{x} is considered merely in the TF domain, where it forms a spectrogram matrix $\mathbf{X} \in \mathbb{C}^{T \times F}$. Therefore the CNN operates on spectrograms and $\hat{\mathbf{X}} = f_{\hat{\theta}}(\mathbf{N})$ for a random but fixed matrix \mathbf{N} . Once $\hat{\mathbf{X}}$ has been established, the time-domain solution is obtained by the inverse STFT.

Regarding the mask, in [18] only the case of completely missing columns of the spectrogram is considered, i.e., for the TF mask $\mathbf{M} \in \{0, 1\}^{T \times F}$ it holds that each column is either full of ones or zeros. Nevertheless, generalization to other TF masks is straightforward. The observed spectrogram \mathbf{X}^{cor} is finally modeled as $\mathbf{X}^{\text{cor}} = \mathbf{M} \odot \mathbf{X}^{\text{orig}}$, where \mathbf{X}^{orig} corresponds to \mathbf{x}^{orig} in the time domain. Note that by analogy with the time-domain case, we have the feasible set $\Gamma_{\text{TF}} = \{\mathbf{X} \mid \mathbf{M} \odot \mathbf{X} = \mathbf{M} \odot \mathbf{X}^{\text{orig}}\}$.

The loss function E in (1), which is optimized with respect to θ , is in the form

$$E = \alpha_1 \text{MSE}(\mathbf{M} \odot \mathbf{X}, \mathbf{X}^{\text{cor}}) + \alpha_2 \text{MSS}(\mathbf{M} \odot \mathbf{X}, \mathbf{X}^{\text{cor}}), \quad (2)$$

where MSS is the multi-scale spectrogram loss [22]. In [18], the weights α_1 and α_2 have values 1 and 0.1 respectively.

B. Architecture

The U-Net is a well-known CNN architecture consisting of several convolutional layers, downsampling (encoder) and upsampling (decoder) operations. In certain applications including audio inpainting, the existence of skip connections between the encoder and decoder stages is important. The authors of [18] used an architecture similar to U-Net called MultiResUNet [23] with an additional inclusion of the so-called harmonic convolution [24], which proved to be the best among multiple tested architectures in [18]. The harmonic convolution is a variation on the common 2D convolution that takes into account higher harmonics of audio.

C. Modifications

The DPAI reconstructs the whole $\hat{\mathbf{X}}$. Yet, considering that only a part of the spectrogram is not known, the authors of [18] evaluate the performance of their method after substituting the coefficients of $\hat{\mathbf{X}}$ that correspond to ones in the mask \mathbf{M} with the observed data. Formally, such an action is a projection

$$\text{proj}_{\Gamma_{\text{TF}}}(\hat{\mathbf{X}}) = \mathbf{M} \odot \mathbf{X}^{\text{cor}} + (\mathbf{1} - \mathbf{M}) \odot \hat{\mathbf{X}} \quad (3)$$

onto the set Γ_{TF} . Note that a resulting sharp transition between the regions is smeared in the time domain due to the nature of the STFT [19]. We call the modified reconstructions *with context*, while the others using the entire $\hat{\mathbf{X}}$ are *without context*.

The other modifications come from the fact that the reconstruction always starts from a random initialization of both θ and \mathbf{N} . As a consequence, the objective and the subjective qualities of the reconstructed signal might slightly vary, based on the particular realization. We observed that averaging the reconstructions from multiple independent reconstructions of the same signal improves the objective performance metrics. Obviously, the cost of such an approach grows linearly with the number of trials. We also noticed that a slight improvement can be assured by averaging a number of final epochs of an individual reconstruction.

In the experimental part, we will study whether the proposed modification of DPAI brings a significant performance improvement.

III. JANSSEN SPECTROGRAM INPAINTING (JANSSEN-TF)

A signal $\mathbf{x} = [x_1, \dots, x_N]^{\top} \in \mathbb{R}^N$ corresponds to an autoregressive process if the following holds:

$$\sum_{i=1}^{p+1} a_i x_{n+1-i} = e_n, \quad n = 1, \dots, N+p, \quad (4)$$

where $\mathbf{a} = [1, a_2, \dots, a_{p+1}]^{\top}$ is the vector of model parameters (AR coefficients), p is the model order, and \mathbf{x} is zero-padded such that its final length is $N+p$. The error term $\mathbf{e} \in \mathbb{R}^{N+p}$ represents a realization of a zero-mean white noise process with variance σ^2 [25, Def. 3.1.2].

In the inpainting method proposed by Janssen et al. [2], the restored audio signal is supposed to follow the AR model (4) while both the missing samples in the time-domain and the unknown AR parameters \mathbf{a} are being estimated. Janssen et al. approach the problem iteratively by repeating two principal steps in the i -th iteration:

- 1) for a temporary solution $\mathbf{x}^{(i)}$, estimate the AR model parameters $\mathbf{a}^{(i)}$;
- 2) given the model parameters $\mathbf{a}^{(i)}$, estimate a new temporary solution $\mathbf{x}^{(i+1)}$ which fits the observed samples and the norm of the model error \mathbf{e} is minimized.

Step 1 can be solved efficiently using standard methods, such as the Durbin–Levinson recursion (see e.g. the function `lpc` in Matlab). Regarding step 2, we propose to adapt the Janssen iteration to the TF setting, denoted Janssen-TF. In our adaptation, the *signal spectrogram* is constrained to fit the observation, \mathbf{X}^{cor} , while the signal follows the estimated AR model. To formalize this modification, note that the error in (4) can be written as $\mathbf{e} = \mathbf{A}\mathbf{x}$, where $\mathbf{A} \in \mathbb{R}^{(N+p) \times N}$ is a Toeplitz matrix composed using the (fixed) coefficients \mathbf{a} . We can then pose the proposed modification of step 2 as

$$\mathbf{x}^{(i+1)} = \arg \min_{\mathbf{x}} \frac{1}{2} \|\mathbf{A}\mathbf{x}\|^2 + \iota_{\Gamma_{\text{TF}}}(\mathbf{L}\mathbf{x}), \quad (5)$$

where $\iota_{\Gamma_{\text{TF}}}$ denotes the indicator function of the convex set Γ_{TF} of feasible spectrograms.³ As such, the problem (5) is convex and it is solvable using standard numerical methods. We propose to employ the alternating direction method of multipliers (ADMM), which includes two principal steps [26, Sec. 3.1.1]:

$$\bar{\mathbf{x}}^{(k+1)} = \arg \min_{\mathbf{x}} \frac{1}{2} \|\mathbf{Ax}\|^2 + \frac{\rho}{2} \|\mathbf{Lx} - \mathbf{z}^{(k)} + \mathbf{u}^{(k)}\|^2, \quad (6a)$$

$$\mathbf{z}^{(k+1)} = \arg \min_{\mathbf{z}} \iota_{\Gamma_{\text{TF}}}(\mathbf{z}) + \frac{\rho}{2} \|\mathbf{L}\bar{\mathbf{x}}^{(k+1)} - \mathbf{z} + \mathbf{u}^{(k)}\|^2. \quad (6b)$$

The whole algorithm is summarized in Alg. 1. For the simplification of (6a), we have posed the assumption⁴ $\mathbf{L}^* \mathbf{L} = \mathbf{I}$, leading to $\bar{\mathbf{x}}^{(k+1)} = \text{prox}_{\frac{1}{2}\|\cdot\|^2}(\mathbf{L}^*(\mathbf{z}^{(k)} - \mathbf{u}^{(k)}))$, see [27, Rem. 3], which then corresponds to line 7 of Alg. 1 [28, Table 1]. Similarly, (6b) boils down to line 8 of the algorithm; this is computed via (3). The hyperparameters of the algorithm are the number of outer and inner iterations (I and K , respectively), and the step size $\rho > 0$.

Algorithm 1: Janssen-TF-ADMM

```

1 initialize  $\mathbf{x}^{(1)}$ 
2 for  $i = 1, \dots, I$  do
3   // AR model update
4    $\mathbf{a}^{(i)} = \text{lpc}(\mathbf{x}^{(i)})$ 
5   // signal update using ADMM
6   form the Toeplitz matrix  $\mathbf{A}$  from  $\mathbf{a}^{(i)}$ 
7    $\mathbf{z}^{(1)} = \mathbf{Lx}^{(i)}, \mathbf{u}^{(1)} = \mathbf{0}$ 
8   for  $k = 1, \dots, K$  do
9      $\bar{\mathbf{x}}^{(k+1)} = (\mathbf{I} + \frac{1}{\rho} \mathbf{A}^\top \mathbf{A})^{-1} \mathbf{L}^*(\mathbf{z}^{(k)} - \mathbf{u}^{(k)})$ 
10     $\mathbf{z}^{(k+1)} = \text{proj}_{\Gamma_{\text{TF}}}(\mathbf{L}\bar{\mathbf{x}}^{(k+1)} + \mathbf{u}^{(k)})$ 
11     $\mathbf{u}^{(k+1)} = \mathbf{u}^{(k)} + \mathbf{L}\bar{\mathbf{x}}^{(k+1)} - \mathbf{z}^{(k+1)}$ 
12  end
13   $\mathbf{x}^{(i+1)} = \bar{\mathbf{x}}^{(K+1)}$ 
14 end

```

Note that several algorithms can be used to solve (5) numerically, such as the primal–dual algorithm [29] or the Douglas–Rachford or the forward–backward algorithms [28], combined with the approximal operator of the function $\iota_{\Gamma_{\text{TF}}}(\mathbf{L} \cdot)$ [30]. However, the variant with ADMM described above, denoted Janssen-TF-ADMM, exhibited the best performance out of six algorithms in our preliminary testing.

IV. EXPERIMENTS

A. Setup and metrics

For our experiments, we adopt the audio dataset⁵ used for the evaluation of DPAI [18]. It consists of 6 music and 2 speech recordings of 5 seconds in length, sampled at 16 kHz. Only minor modifications were made to the original distribution of gaps (i.e., the placement of the missing spectrogram columns), such that each test excerpt includes

³Note that the original Janssen algorithm minimizes the function $\frac{1}{2} \|\mathbf{Ax}\|^2 + \iota_{\Gamma_{\text{TF}}}(\mathbf{x})$ in subproblem 2.

⁴This assumption is met for instance if \mathbf{L} corresponds to a Parseval tight frame, which can be ensured by a suitable setting of the STFT.

⁵<https://github.com/fmiotello/dpai/>

5 gaps of the same length. The gap lengths range from 1 up to 6 missing columns. In turn, the entire test set comprises of $8 \times 6 = 48$ corrupted audio signals. Even though the dataset is relatively small and includes only a few types of audio signals, we decided to stick to it because its use justifies a fair comparison of the proposed method with DPAI. The choice allows the use of exactly the same U-net architecture of DPAI from [18]. In particular, we choose their “best2” setting. The number of epochs of the Adam optimizer is 5000.

The STFT (i.e., the operator \mathbf{L}) utilizes the 2048-sample-long Hann window (which corresponds to 128 ms), with 75% overlap and 2048 frequency channels; this setting is the default for the time-frequency transform of the librosa package⁶, as used in [18], and ensures that \mathbf{L} forms a Parseval tight frame.

To objectively evaluate the reconstruction quality, we assess the difference between the inpainted signal $\hat{\mathbf{x}}$ and a clean reference \mathbf{x}^{orig} using two standard metrics:

- 1) signal-to-noise ratio (SNR), defined in decibels as $\text{SNR}(\hat{\mathbf{x}}, \mathbf{x}^{\text{orig}}) = 10 \log_{10} \frac{\|\mathbf{x}^{\text{orig}}\|^2}{\|\mathbf{x}^{\text{orig}} - \hat{\mathbf{x}}\|^2}$ [3],
- 2) objective difference grade (ODG) computed using the PEMO-Q [31], which takes psychoacoustics into account and predicts the subjective evaluation of the difference between $\hat{\mathbf{x}}$ and \mathbf{x}^{orig} on the scale from -4 to 0 (from “very annoying” to “imperceptible”).

Above that, we run

- 3) a subjective listening test containing a limited number of excerpts. The MUSHRA-type test [32] was performed that includes the reference signal, the DPAI reconstruction with context, the DPAI reconstruction without context, the DPAI with context but averaged result from four random initializations, the gapwise Janssen method in the time domain [12], the Janssen-TF-ADMM, and finally the hidden anchor, i.e., the signal reconstructed from the spectrogram with gaps.

The participants were asked to score the perceived similarity of the signals with the reference on a continuous scale from 0 to 100, with the help of the webMUSHRA environment⁷. The test was run in a quiet music studio, using a professional sound card and headphones. The listening conditions were identical for all the participants. Following the recommendation [32], 11 assessors out of 18 were selected through post-screening.

B. Results

First, we evaluate the proposed modifications of DPAI. As seen in Fig. 1, averaging the realizations brings improvement in quality in terms of SNR, but it comes at the cost of a higher time complexity. The differences observed in Fig. 1 were further tested using the Wilcoxon signed rank test⁸, which proved that the median of the SNR using DPAI with averaging is significantly higher compared to the original DPAI with context. On the other hand, a significant difference in case of the ODG metric has not been proven.

⁶<https://librosa.org/doc/0.10.2/generated/librosa.stft.html>

⁷<https://github.com/audiolabs/webMUSHRA/>

⁸<https://www.mathworks.com/help/stats/signrank.html>

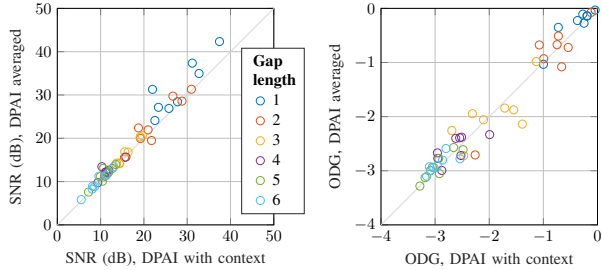


Fig. 1. Comparison of DPAI reconstruction with context versus the proposed DPAI variant averaging four random initializations.

In contrast to the averaging of realizations, the averaging across the final epochs from a single realization does not increase the computational load and brings better quality mostly to audio recordings reconstructed without context—the greatest improvement (averaged over test signals) was 0.16 ODG for the gap of 2 columns and 15 epochs averaged. However, this strategy has a negligible impact when considering reconstructions *with context*.

The objective comparison that includes the proposed Janssen-TF method is shown in Fig. 2. The first observation is that the time-domain-based Janssen method [12] cannot compete with the other methods. This is due to the incompatibility of gaps in the time and time-frequency domains (a sharp mask in the spectrogram domain affects a longer signal portion when transformed into the time domain). While the average performance of the DPAI variants mostly lie within the confidence intervals of each other, suggesting limited significance of the differences, the proposed Janssen-TF-ADMM method largely outperforms the competitors in both SNR and ODG (except for the longest gaps).

To support the objective evaluation, Fig. 3 presents the results of the subjective listening test. Its results correlate well with the objective evaluation; in particular, Janssen-TF-ADMM is superior to the competing methods. Moreover, this result is statistically significant in terms of medians. On the other hand, the DPAI variants scored almost the same. This is in line with the ODG results in Fig. 1, even though the listening test featured only a selection of the test signals.

A single run of DPAI takes ca 19 minutes on the NVIDIA Tesla V100S GPU with 32 GB of memory, regardless the number of missing spectrogram columns. Computing a single signal with Janssen-TF-ADMM takes 10 to 20 minutes, directly proportional to the number of columns; this corresponds to a PC with Intel Core i7 3.40 GHz processor, 32 GB RAM.

V. CONCLUSION AND OUTLOOK

The paper has shown that the proposed method of spectrogram inpainting, Janssen-TF, performs significantly better than the recently introduced DPAI algorithm, which is based on the deep prior idea. This conclusion has been certified both by objective and subjective tests. The proposed minor modifications of DPAI led to a slight improvement in terms of the SNR, but have not been reflected in the perceived sound quality.

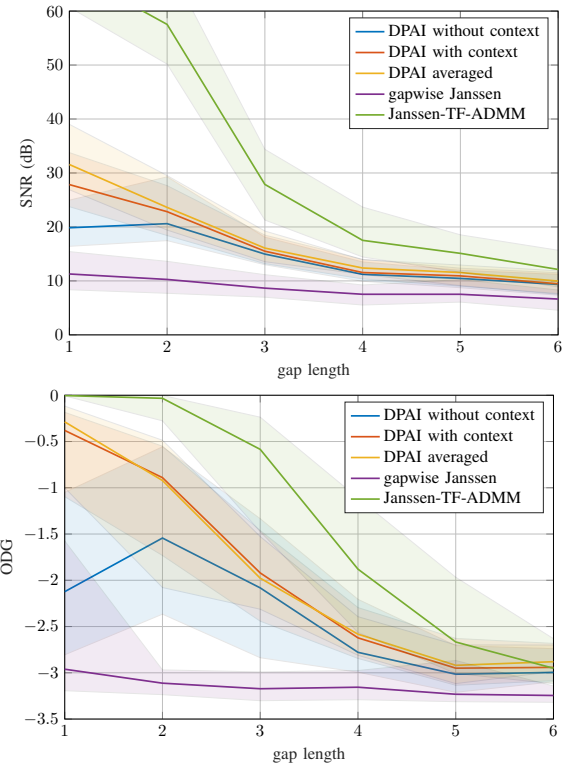


Fig. 2. Comparison of the inpainting methods using objective metrics – SNR (top) and ODG (bottom). The plots show results averaged over the 8 test signals together with the bootstrap interval estimates of the mean values at the $\alpha = 5\%$ significance level [33, p. 160]. If the intervals do not overlap, it may be concluded that the difference of the means is statistically significant.

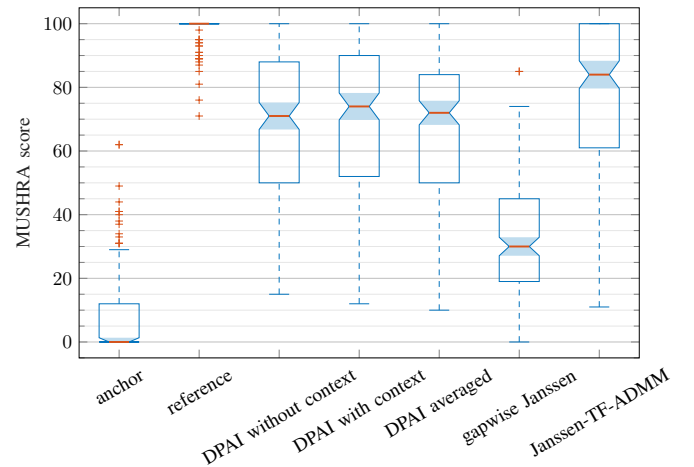


Fig. 3. A boxplot showing the distribution of scores in the listening test. The individual boxes span from the 25th to the 75th percentile of the recorded scores. The notches (filled areas) around the medians (orange lines) are constructed such that boxes whose notches do not overlap have different medians at the 5% statistical significance level.

In the future, it might be interesting to use the same adaptation strategy with other methods for the time-domain inpainting, such as the PHAIN regularized algorithm [13].

Matlab source codes for Janssen-TF and other supplementary material are publicly available at <https://github.com/rajmic/spectrogram-inpainting>.

REFERENCES

- [1] W. Etter, "Restoration of a discrete-time signal segment by interpolation based on the left-sided and right-sided autoregressive parameters," *IEEE Transactions on Signal Processing*, vol. 44, no. 5, pp. 1124–1135, 1996.
- [2] A. J. E. M. Janssen, R. N. J. Veldhuis, and L. B. Vries, "Adaptive interpolation of discrete-time signals that can be modeled as autoregressive processes," *IEEE Trans. Acoustics, Speech and Signal Processing*, vol. 34, no. 2, pp. 317–330, Apr. 1986.
- [3] Amir Adler, Valentin Emiya, Maria G. Jafari, Michael Elad, Rémi Grisonval, and Mark D. Plumley, "Audio Inpainting," *IEEE Transactions on Audio, Speech, and Language Processing*, vol. 20, no. 3, pp. 922–932, Mar. 2012.
- [4] Ondřej Mokrý and Pavel Rajmic, "Audio inpainting: Revisited and reweighted," *IEEE/ACM Transactions on Audio, Speech, and Language Processing*, vol. 28, pp. 2906–2918, 2020.
- [5] Ondřej Mokrý, Pavel Záviška, Pavel Rajmic, and Vítězslav Veselý, "Introducing SPAIN (SParse Audio INpainter)," in *2019 27th European Signal Processing Conference (EUSIPCO)*. 2019, IEEE.
- [6] Ondřej Mokrý, Paul Magron, Thomas Oberlin, and Cédric Févotte, "Algorithms for audio inpainting based on probabilistic nonnegative matrix factorization," *Signal Processing*, p. 10, dec 2022.
- [7] Yuval Bahat, Yoav Y. Schechner, and Michael Elad, "Self-content-based audio inpainting," *Signal Processing*, vol. 111, no. 0, pp. 61–72, 2015.
- [8] Ichraak Toumi and Valentin Emiya, "Sparse non-local similarity modeling for audio inpainting," in *2018 IEEE International Conference on Acoustics, Speech and Signal Processing (ICASSP)*. Apr. 2018, IEEE.
- [9] Nathanael Perraudin, Nicki Holighaus, Piotr Majdak, and Peter Balazs, "Inpainting of long audio segments with similarity graphs," *IEEE/ACM Transactions on Audio, Speech, and Language Processing*, pp. 1–1, 2018.
- [10] Gal Greshler, Tamar Shaham, and Tomer Michaeli, "Catch-A-Waveform: Learning to generate audio from a single short example," in *Advances in Neural Information Processing Systems*, M. Ranzato, A. Beygelzimer, Y. Dauphin, P. S. Liang, and J. Wortman Vaughan, Eds. 2021, vol. 34, pp. 20916–20928, Curran Associates, Inc.
- [11] Eloi Moliner, Jaakko Lehtinen, and Vesa Välimäki, "Solving audio inverse problems with a diffusion model," in *2023 IEEE International Conference on Acoustics, Speech and Signal Processing (ICASSP)*. jun 2023, IEEE.
- [12] Ondřej Mokrý and Pavel Rajmic, "On the use of autoregressive methods for audio inpainting," Mar. 2024.
- [13] Tomoro Tanaka, Kohei Yatabe, and Yasuhiro Oikawa, "Phase-aware audio inpainting based on instantaneous frequency," in *2021 Asia-Pacific Signal and Information Processing Association Annual Summit and Conference (APSIPA ASC)*, 2021, pp. 254–258.
- [14] Marie Daňková, Pavel Rajmic, and Radovan Jiřík, "Acceleration of perfusion MRI using locally low-rank plus sparse model," in *Latent Variable Analysis and Signal Separation*, Liberec, 2015, pp. 514–521, Springer.
- [15] P. Rajmic, Z. Koldovský, and M. Daňková, "Fast reconstruction of sparse relative impulse responses via second-order cone programming," in *IEEE Workshop on Applications of Signal Processing to Audio and Acoustics (WASPAA'17)*, New Paltz, NY, USA, Oct. 2017.
- [16] Andrés Marafioti, Nathanaël Perraudin, Nicki Holighaus, and Piotr Majdak, "A context encoder for audio inpainting," *IEEE/ACM Transactions on Audio, Speech, and Language Processing*, vol. 27, no. 12, pp. 2362–2372, Dec. 2019.
- [17] Andrés Marafioti, Piotr Majdak, Nicki Holighaus, and Nathanaël Perraudin, "GACELA: A generative adversarial context encoder for long audio inpainting of music," *IEEE Journal of Selected Topics in Signal Processing*, vol. 15, no. 1, pp. 120–131, Jan. 2021.
- [18] Federico Miotello, Mirco Pezzoli, Luca Comanducci, Fabio Antonacci, and Augusto Sarti, "Deep Prior-Based Audio Inpainting Using Multi-Resolution Harmonic Convolutional Neural Networks," *IEEE/ACM Transactions on Audio, Speech, and Language Processing*, pp. 1–11, 2023.
- [19] Pavel Rajmic, Hana Bartlová, Zdeněk Průša, and Nicki Holighaus, "Acceleration of audio inpainting by support restriction," in *2015 7th International Congress on Ultra Modern Telecommunications and Control Systems and Workshops (ICUMT)*. Oct. 2015, pp. 325–329, IEEE.
- [20] Dmitry Ulyanov, Andrea Vedaldi, and Victor Lempitsky, "Deep image prior," *International Journal of Computer Vision*, vol. 128, no. 12, 2020.
- [21] Diederik P. Kingma and Jimmy Ba, "Adam: A method for stochastic optimization," 2014.
- [22] Ryuichi Yamamoto, Eunwoo Song, and Jae-Min Kim, "Parallel wagan: A fast waveform generation model based on generative adversarial networks with multi-resolution spectrogram," in *2020 IEEE International Conference on Acoustics, Speech and Signal Processing*, Spain, 2020, pp. 6199–6203, IEEE.
- [23] Nabil Ibtehaz and M. Sohel Rahman, "Multiresunet : Rethinking the unet architecture for multimodal biomedical image segmentation," *Neural Networks*, vol. 121, pp. 74–87, 2020.
- [24] Hirotoshi Takeuchi, Kunio Kashino, Yasunori Ohishi, and Hiroshi Saruwatari, "Harmonic lowering for accelerating harmonic convolution for audio signals," 10 2020, pp. 185–189.
- [25] Peter J. Brockwell and Richard A. Davis, *Time Series: Theory and Methods*, Springer series in statistics. Springer, 2 edition, 2006.
- [26] Stephen P. Boyd, Neal Parikh, Eric Chu, Borja Peleato, and Jonathan Eckstein, "Distributed optimization and statistical learning via the alternating direction method of multipliers," *Foundations and Trends in Machine Learning*, vol. 3, no. 1, pp. 1–122, 2011.
- [27] Pavel Záviška, Ondřej Mokrý, and Pavel Rajmic, "S-SPADE Done Right: Detailed Study of the Sparse Audio Declipper Algorithms," *techreport*, Brno University of Technology, Sept. 2018.
- [28] P.L. Combettes and J.C. Pesquet, "Proximal splitting methods in signal processing," *Fixed-Point Algorithms for Inverse Problems in Science and Engineering*, vol. 49, pp. 185–212, 2011.
- [29] Antonin Chambolle and Thomas Pock, "A first-order primal-dual algorithm for convex problems with applications to imaging," *Journal of Mathematical Imaging and Vision*, vol. 40, no. 1, pp. 120–145, 2011.
- [30] Ondřej Mokrý and Pavel Rajmic, "Approximal operator with application to audio inpainting," *Signal Processing*, vol. 179, pp. 107807, 2021.
- [31] R. Huber and B. Kollmeier, "PEMO-Q—A new method for objective audio quality assessment using a model of auditory perception," *IEEE Trans. Audio Speech Language Proc.*, vol. 14, no. 6, pp. 1902–1911, Nov. 2006.
- [32] "Recommendation ITU-R BS.1534-3: Method for the subjective assessment of intermediate quality level of audio systems," 2015.
- [33] Bradley Efron and Robert J. Tibshirani, *An Introduction to the Bootstrap*, Chapman & Hall, New York, 1994.